Transient X-Ray Fragmentation: Probing a Prototypical Photoinduced Ring Opening

Vladimir S. Petrović,[1,2,*] Marco Siano,[3] James L. White,[2,4] Nora Berrah,[5] Christoph Bostedt,[6] John D. Bozek,[6] Douglas Broege,[2,4] Max Chalfin,[1,2] Ryan N. Coffee,[6] James Cryan,[1,2] Li Fang,[5] Joseph P. Farrell,[1,2] Leszek J Frasinski,[3] James M. Glownia,[2,4] Markus Gühr,[2] Matthias Hoener,[5] David M. P. Holland,[7] Jaehee Kim,[1,2] Jonathan P. Marangos,[3] Todd Martinez,[2,8] Brian K. McFarland,[2,4] Russell S. Minns,[9] Shungo Miyabe,[2,8] Sebastian Schorb,[6] Roseanne J. Sension,[10] Limor S. Spector,[1,2] Richard Squibb,[3] Hongli Tao,[2,8] Jonathan G. Underwood,[9] and Philip H. Bucksbaum[1,2,4]

[1]*Stanford University, Department of Physics, Stanford, California 94305, USA*
[2]*The PULSE Institute, SLAC, Menlo Park, California 94025, USA*
[3]*Blackett Laboratory, Imperial College London, London, United Kingdom*
[4]*Stanford University, Department of Applied Physics, Stanford, California 94305, USA*
[5]*Physics Department, Western Michigan University, Kalamazoo, Michigan 49008, USA*
[6]*LCLS at SLAC National Accelerator Laboratory, Menlo Park, California 94025, USA*
[7]*Photon Science Department, Daresbury Laboratory, Warrington, United Kingdom*
[8]*Stanford University, Department of Chemistry, Stanford, California 94305, USA*
[9]*Department of Physics and Astronomy, University College London, London, United Kingdom*
[10]*Department of Chemistry, Department of Physics, University of Michigan, Ann Arbor, Michigan 48109, USA*
(Received 28 December 2011; published 21 June 2012)

We report the first study of UV-induced photoisomerization probed via core ionization by an x-ray laser. We investigated x-ray ionization and fragmentation of the cyclohexadiene-hexatriene system at 850 eV during the ring opening. We find that the ion-fragmentation patterns evolve over a picosecond, reflecting a change in the state of excitation and the molecular geometry: the average kinetic energy per ion fragment and H^+-ion count increase as the ring opens and the molecule elongates. We discuss new opportunities for molecular photophysics created by optical pump x-ray probe experiments.

DOI: 10.1103/PhysRevLett.108.253006 PACS numbers: 33.15.−e, 31.50.Gh, 32.80.Hd, 33.20.Rm

X-ray pulses with duration from 200 fs to below 5 fs are now available at Linac Coherent Light Source at the SLAC National Accelerator Laboratory at Stanford University (LCLS at SLAC) [1]. The advent of free-electron lasers (FEL) with high fluence and short x-ray pulses has had an early impact on AMO science [2–9]. This source is a powerful new probe of molecular dynamics in the gas phase. The primary uses envisioned for LCLS rely on scattering, diffraction, and resonant absorption of x rays. We describe a technique that does not require a *resonant* x-ray field and thus permits a study of species that have absorption edges outside of the energy range currently available at LCLS, including carbon-containing molecules. In optical pump x-ray probe (OPXP) time-resolved experiments an optical pulse initiates a reaction that is then monitored by time-resolved x-ray–induced ionization and fragmentation. The ion-fragmentation patterns encode information about instantaneous molecular geometry and motion. We have used time-resolved x-ray ionization and fragmentation to probe transient structures of an isomerizing molecule by applying the OPXP method for the first time, in the case of 1,3-cyclohexadiene. In our case a UV pulse initiates ring opening and as the ring opens a delayed x-ray pulse starts to fragment the molecule, providing information about the isomerization. Our results show that x-ray ionization and fragmentation is capable of detecting the evolution of transient molecular species.

The unique opportunities of this new powerful way of probing molecular dynamics arise from the potential for very short x-ray durations ($\approx$ 1 fs) [10]. Furthermore, in contrast to optical lasers that perform fragmentation through valence electron stripping, followed by Coulomb explosion (CE), the initial interaction with x rays involves unperturbed core electrons localized at atomic sites. This creates a structural probe that does not perturb the valence electrons and has the potential for atomic specificity.

In a prototypical Coulomb-explosion experiment, several electrons are stripped away from a molecule on a time scale faster than the nuclear motion [11]. The remaining positive charges repel each other and the kinetic energy release (KER) of the ions is a measure of the distance between the positive charges before they started moving, providing information for reconstruction of the molecular geometry. Development of short laser pulses, which could be focused to produce fields capable of fragmenting molecules, provided a path for inducing Coulomb explosion with an advantage over foil experiments [12–14], of permitting synchronization in pump-probe experiments. This enabled Coulomb explosions to monitor wave packet evolution [11,15,16]. Intense laser field fragmentation has been used to monitor the photoisomerization between 1,3-cyclohexadiene and 1,3,5-hexatriene (CHD and HT, respectively), where ionic resonances in intense IR field

 © 2012 American Physical Society

fragmentation create differences in ion-fragment time-of-flight (TOF) spectra of the two species [17].

Although much has been learned from these experiments, the interaction with an IR field extends over the entire molecule and can lead to many parallel processes in the strong-field regime, including molecular alignment, above threshold ionization (ATI), multiphoton ionization, bond softening, enhanced ionization, and wave packet interception [18]. The ponderomotive energy of the laser field is typically many eV, whereas the ponderomotive energy of the x-ray field is negligible. The cross section for x-ray ionization does not depend strongly on interatomic separation. X-ray fragmentation of a molecule provides a virtually "field-free" probe of the transformation. This is because the interaction with the x-ray field occurs predominantly through core electrons and results in localized charge imbalance. The relaxation of a core-ionized system occurs either by emission of a photon, or, more likely in the case of light nuclei, by ejection of one or more Auger electrons on the time scale of a few fs. The leftover excess energy is distributed over the internal degrees of freedom of the remaining dication that rapidly fragments due to the repulsion between the remaining positive charges. Absorption of a single x-ray photon deposits a large amount of energy in the molecule, which then leads to ionization and fragmentation, while in the optical strong-field regime many photons need to be absorbed to reach the fragmenting dication. The kinetic energy carried by the positively charged fragments is expected to depend on the excitation state of the molecule prior to fragmentation. Intense laser field fragmentation necessarily operates in a nonlinear regime, and the fragmentation patterns depend strongly on the characteristics of the pulse [19,20], while for the case of x-ray fragmentation performed in the linear regime the ion-fragmentation patterns should not depend on x-ray intensity.

The molecule 1,3-cyclohexadiene is a small hydrocarbon ring, C_6H_8, which undergoes a large structural change upon photoexcitation. Absorption of one UV photon leads in CHD to ring opening and molecular extension (see inset in Fig. 1). This process has been extensively studied, in part because of its role in vitamin D biosynthesis. Time-resolved pump-probe techniques have been employed to understand this process [20–25]. These studies have found that the conical intersection-mediated ring-opening step in isomerization is completed in less than 200 fs [22], after which the molecule undergoes conformational changes on a range of time scales (see inset in Fig. 1) [26,27].

We observe a clear signature of the isomerization in the fragmentation signal. The KER and number of H^+ ion fragments per molecule evolve over ≈ 1 ps in our experiment.

The experiment was performed in the high-field physics chamber in the AMO experimental end station at the LCLS at SLAC [28]. The CHD sample was brought into the gas

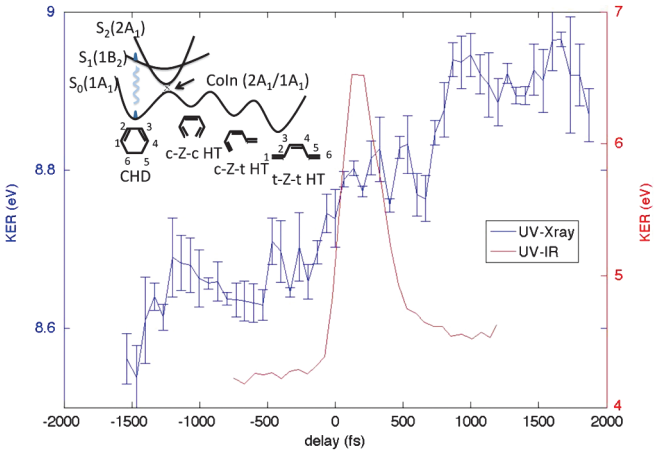

FIG. 1 (color). Average kinetic energy per fragment as a function of time delay after the UV excitation in UV x ray (blue, left axis) and UV IR (red, right axis) CHD ring-opening experiments. The inset shows the electronic states of the CHD-HT pair discussed in the text.

phase by flowing ≈ 200 mbar He through liquid CHD (vapor pressure ≈ 10 mbar). During the search for the overlap between the IR and x-ray pulses we switched the sample to N_2. A 50 μJ, 266 nm (≈ 4.7 eV), ≈ 50 fs pump pulse focused to 150 μm diameter launched a wave packet onto the spectroscopically bright 1B potential energy surface of CHD (see inset on Fig. 1). Following a ≈ 55 fs nonradiative transition to the $2A$ state [22], the wave packet accelerates toward a conical intersection between the $2A$ state and the ground $1A$ state from where it can continue toward either the CHD or HT potential energy wells. The x-ray photon energy of 850 eV, well above the $1s$ ionization threshold for carbon, was selected for the most stable of the operation of the LCLS. The x-ray and UV pulses propagated collinearly, and crossed the molecular beam at the right angle. This x-ray pulse (< 70 fs) arrived at a variable delay after the UV pulse and core ionized the isomerizing molecule. The molecule subsequently fragments. Ion fragments were collected at 60 Hz, 500 shots per delay point before shot-rejection based on the x-ray intensity and sample pressure. We operated in the weak focusing regime for the x rays, in order to avoid nonlinear processes [3,6] (see Fig I in the Supplemental Material [29]). The spot size was 30×50 μm (horizontal and vertical directions, respectively). We used a velocity-map imaging detector (VMI) to collect some of the data [30], and a separate high-resolution ion-TOF spectrometer in other runs. More experimental details are given in the Supplemental Material [29].

The jitter in timing between the x rays and optical laser pulses, which had multiple contributions, is the principal limit to time resolution of the experiment. X-ray jitter corrections based on phase-cavity arrival measurements of the electron bunch in the accelerator were collected simultaneously and applied to pump-probe data in

postprocessing, as has been done previously [2]. The overall time resolution of our experiment was ≈ 300 fs.

Temporal and spatial overlap of the pump and probe laser pulses was accomplished by observing the cross correlation between a strong 800 nm pulse, which was well synchronized with the ultraviolet pulse laser, and the x rays in the ion-fragmentation spectra of N_2. In particular, we monitored the 800 nm-dissociation of nitrogen molecular dications produced by the x rays [2]. The overlap between the IR and UV pulses was found by observing the transient peak in H^+ produced by IR fragmentation of UV-excited CHD. This peak is known to occur approximately 200 fs after UV excitation [22]. Overlap of the 800 nm and x rays combined with overlap of 800 nm beam and UV beam does not guarantee overlap of the UV beam with the x-ray beam, so this report is limited to two data runs where postprocessing indicates that we had the requisite UV–x-ray overlap. We observed that over hours stepwise shifts in time zero can occur. Such shifts can be seen in comparison of the time zero in Figs. 1 and 2.

In the UV x-ray time-delay scan monitored with the VMI detector we observed a variation with time delay of the fragment radial momentum distribution following the UV excitation, see Fig. 1. We also observe an increase in the ion count upon UV excitation. This increase in the ion count agrees with an increase in the H^+ count observed in a separate set of measurements that used the ion-TOF detector under the same UV–x-ray overlap conditions, see Fig. 2. In neither of the two cases can the observed changes in the H^+ ion count and average ion KER upon the UV excitation be explained by systematic variations of the x-ray intensity, UV laser intensity, or the gas pressure.

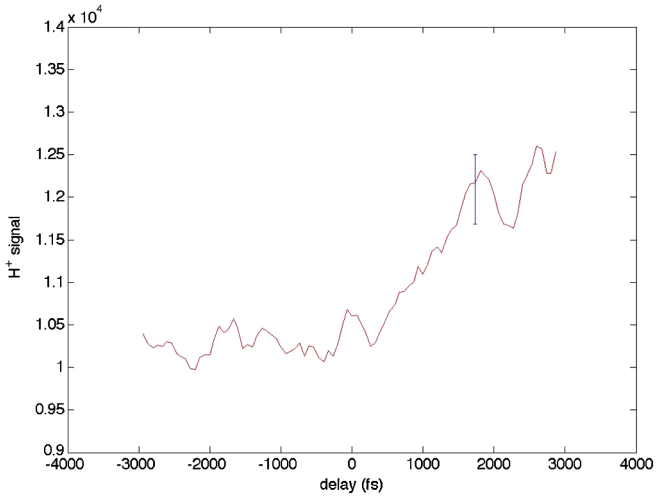

FIG. 2 (color online). Time dependence of the H^+ ion count after the UV excitation (recorded using an ion-TOF detector) plotted as an error-weighted average over 335 fs window. Stepwise temporal drifts, which occur over hours, can be seen in comparison of time zero in Figs. 1 and 2.

We conclude that the observed effects are caused by evolution of the molecule following UV excitation.

The VMI image centering for different pump-probe delays is described in the Supplemental Material [29]. We selected the acquisition events for which the x-ray pulse energy was within the narrow range of 0.95–1.10 mJ/pulse, to reduce the possibility of systematic bias due to a poorly characterized x-ray source. Similarly, to avoid bias due to pressure changes during the pump-probe scan, we only selected the portion of the data where the chamber pressure was $1.400 \pm 0.005.10^{-7}$ Torr. Averaged VMI images for each time bin were inverted using an onion-peeling algorithm [31]. A plot of the radial distribution of the ion counts as a function of the UV–x-ray delay after inversion is given in the Supplemental Material [29]. The kinetic energy distribution vs time delay was obtained after a radius-to-energy calibration using a SIMION simulation for the experimental geometry and voltages.

From the shot-averaged velocity-map images we extracted the evolution of the average ion-KER per fragment with the UV x-ray delay, shown in Fig. 1. The initial increase of the average KER per fragment around the time when the two pulses temporally overlap is followed by a further increase to a plateau value after which the average KER does not change within the temporal window of our measurement. Only a fraction of the UV-excited molecules is probed by the x-ray pulse, so the magnitude of the increase in the kinetic energy per fragment in Fig. 1 is reduced due to signal dilution by molecules that fragment following x-ray absorption, but have not absorbed a UV photon. Despite the limitations in signal-to-noise arising from a background of unexcited molecules and time resolution limited by pump-probe jitter OPXP can clearly detect molecular transformations.

We also explored the number of fragment ions per molecule using an ion-TOF detector (see Fig. 2). The ion with the most significant change in abundance following UV excitation is H^+. Figure 2 includes all acquisition events with x-ray pulse intensity larger than 0.1 mJ, and the data are normalized by x-ray pulse energy, following background subtraction. An increase in the production of H^+ in HT compared to CHD had also been observed in x-ray fragmentation experiments on the stable CHD and HT isomers (a mixture of *tZt* and *tEt* forms in case of HT), performed at the Advanced Light Source synchrotron (to be published separately [32], also see Fig. IV in the Supplemental Material [29]), although in that case the increase in the H^+ count was smaller than observed in the time-resolved experiment. Since geometry change by itself does not account for the magnitude of the signal change, we deduce that the change in the kinetic energy of the nuclei contributes to the signal as well. This comparison suggests that transient or vibrationally hot molecules possess a fragmentation spectrum that is richer in H^+.

The relative change in the ion-KER from before to after UV excitation should in principle provide information about the evolution of the geometry and the kinetic energy of the nuclei during the isomerization. In the x-ray experiment the kinetic energy and the ion count increase on a time scale considerably longer than electronic excitation, but consistent with subsequent conformational changes that the excited molecule undergoes after the ring opening [26,27] and possible reactions of hot product and educt in the ground state [33]. At present, it is difficult to separate different contributions to the observed signal. In contrast, the ion-KER evolution in the IR-fragmentation signal (red curve in Fig. 1; recorded under the same conditions), is dominated by valence electronic resonance effects around 200 fs [20,34]. An important difference between the strong IR field fragmentation and x-ray fragmentation at 850 eV is the inability of the latter one to ionize neutral hydrogen fragments.

In a molecule containing light elements such as carbon, the primary path for deexcitation following x-ray core ionization is Auger decay, which populates multiple excited states of the dication. In CHD, similar to other small hydrocarbons [35], innervalence excited states play an important role, and dication created by the Auger transition can be left with many eV of energy excess with respect to its ground state (see Fig. V in the Supplemental Material [29]). Such highly excited states are nonetheless incapable of further Auger decay because the ionization potential from the dication to the trication is still larger than the excitation energy. The primary path for the excess energy removal is through molecular fragmentation, which is expected to occur much faster than a radiative decay.

The observed variation of the KER upon photoexcitation can be related to the variation along the reaction path of the dicationic states created by the Auger transition. Our calculation, described in the Supplemental Material [29] and Ref. [36], demonstrates that the distribution of the dicationic states created by the Auger transition is geometry- and excitation dependent. This results in a variation of the excess fragmentation energy during the isomerization. Furthermore, these dicationic states have potential energy surfaces (PES) with geometries significantly different than those of the neutral and singly charged ion. As the momentum is conserved in the transitions, the evolution on the dicationic potential energy surfaces is governed by the momentum accumulated on both the neutral and singly charged PES.

Most of the momentum is gained in Coulomb explosion on the PES of the doubly charged cation. The momentum on the neutral PES is gained as a result of the evolution on the 1B, 2A, and 1A states, following the UV excitation. It is usually assumed that upon core excitation the momentum change on the singly charged PES is negligible prior to the Auger transition onto the PES of the doubly charged ion. However, in species that contain lighter atoms with longer Auger lifetimes (≈ 6 fs in C) [37], especially bonded to lighter atoms such as H, a significant impulse due to the reduction in nuclear screening upon core excitation can result in an increase of the C-H bond length during the core-hole lifetime, resulting in easier detachment of that hydrogen during the subsequent fragmentation. This is further discussed in the Sec. 9 of the Supplemental Material [29].

Our results point toward the need to model the x-ray fragmentation of electronically excited small molecules. This requires a calculation of Auger rates of evolving species, and accurate modeling of wave packet motion on many potential energy surfaces, where the fragmentation branching ratios are sensitive to individual barrier heights [38]. However, a simple calculation of the purely-electronic contribution to the effect of the excitation and geometry on the distribution of the dicationic states in a single-orbital approximation provides some information about these interesting dynamics.

We have shown that time-resolved x-ray ionization and fragmentation is capable of probing transient molecular structures. X rays perturb the bonding electrons only weakly compared to intense IR laser pulses, which makes x rays suitable for probing rapidly evolving transient species. This technique has a potential for elemental specificity and shorter probing times (≈ 1 fs). It is especially well suited for molecules with lighter atoms where the excess energy necessarily leads to molecular fragmentation. In CHD we observe that the kinetic energy and the H^+ ion production per molecule are higher in the photoexcited molecule. The evolution of the ion-fragmentation patterns in CHD happens over a picosecond, considerably longer than the duration of the electronic excitation, but consistent with conformational changes and subsequent reactions that the hot ground-state molecule undergoes [26,27,33]. The method will greatly benefit from improvements in time resolution, through better optical-laser–FEL synchronization, and higher statistics through greater availability of ultrafast x-ray pulses. We anticipate that x-ray fragmentation experiments will spur interest to model the evolution of the Auger-electron and ion-KER spectra of molecules in excited states.

This work was carried out in the Stanford PULSE Institute through the support of the National Science Foundation. Some of the collaborators in this paper received their support through the SLAC National Accelerator Laboratory, Chemical Sciences, Bio and Geosciences Division of the Office of Basic Energy Sciences, U.S. Department of Energy, UK EPSRC via EP/F021232/1 and EP/E028063/1 and the STFC. Portions of this research were carried out at the Linac Coherent Light Source (LCLS) at the SLAC National Accelerator Laboratory. LCLS is an Office of Science User Facility operated for the U.S. Department of Energy Office of Science by Stanford University. Portions of this

research were carried out at the Advanced Light Source (ALS) at the Lawrence Berkeley National Laboratory. The Advanced Light Source is supported by the Director, Office of Science, Office of Basic Energy Sciences, of the U.S. Department of Energy under Contract No. DE-AC02-05CH11231.

*petrovic@stanford.edu

[1] https://slacportal.slac.stanford.edu/sites/lclscore_public/Lists/LCLS_FAQ/FAQ.aspx.
[2] J. M. Glownia *et al.*, Opt. Express **18**, 17 620 (2010).
[3] J. Cryan *et al.*, Phys. Rev. Lett. **105**, 083004 (2010).
[4] L. Young *et al.*, Nature (London) **466**, 56 (2010).
[5] N. Berrah *et al.*, J. Mod. Opt. **57**, 1015 (2010).
[6] M. Hoener *et al.*, Phys. Rev. Lett. **104**, 253002 (2010).
[7] L. Fang *et al.*, Phys. Rev. Lett. **105**, 083005 (2010).
[8] G. Doumy *et al.*, Phys. Rev. Lett. **106**, 083002 (2011).
[9] S. Hau-Riege *et al.*, Phys. Rev. Lett. **105**, 043003 (2010).
[10] Y. Ding *et al.*, Phys. Rev. Lett. **102**, 254801 (2009).
[11] C. Ellert, H. Stapelfeldt, E. Constant, H. Sakai, J. Wright, D. M. Rayner, and P. B. Corkum, Phil. Trans. R. Soc. A **356**, 329 (1998).
[12] L. J. Frasinski, K. Codling, P. Hatherly, J. Barr, I. N. Ross, and W. T. Toner, Phys. Rev. Lett. **58**, 2424 (1987).
[13] K. Codling, L. J. Frasinski, P. Hatherly, and J. R. M. Barr, J. Phys. B **20**, L525 (1987).
[14] Z. Vager, R. Naaman, and E. Kanter, Science **244**, 426 (1989).
[15] C. Cornaggia, Laser Phys. **19**, 1660 (2009).
[16] F. Légaré, K. F. Lee, A. D. Bandrauk, D. M. Villeneuve, and P. B. Corkum, J. Phys. B **39**, S503 (2006).
[17] W. Fuß, T. Schikarski, W. E. Schmid, S. A. Trushin, P. Hering, and K. L. Kompa, J. Chem. Phys. **106**, 2205 (1997).
[18] T. Brabec, *Strong Field Laser Physics*, Springer Series in Optical Sciences (Springer, New York, 2008).
[19] X. P. Tang, A. Becker, W. Liu, S. M. Sharifi, O. G. Kosareva, V. P. Kandidov, P. Agostini, and S. L. Chin, Appl. Phys. B **80**, 547 (2005).
[20] J. L. White, J. Kim, V. S. Petrović, and P. H. Bucksbaum, J. Chem. Phys. **136**, 054303 (2012).
[21] M. Merchán, L. Serrano-Andrés, L. S. Slater, B. O. Roos, R. McDiarmid, and X. Xing, J. Phys. Chem. A **103**, 5468 (1999).
[22] K. Kosma, S. A. Trushin, W. Fuß, and W. E. Schmid, Phys. Chem. Chem. Phys. **11**, 172 (2009).
[23] M. Kotur, T. Weinacht, B. J. Pearson, and S. Matsika, J. Chem. Phys. **130**, 134311 (2009).
[24] E. C. Carroll, B. J. Pearson, A. C. Florean, P. H. Bucksbaum, and R. J. Sension, J. Chem. Phys. **124**, 114506 (2006).
[25] H. Ihee, V. A. Lobastov, U. M. Gomez, B. M. Goodson, R. Srinivasan, C.-Y. Ruan, and A. H. Zewail, Science **291**, 458 (2001).
[26] S. Lochbrunner, W. Fuss, W. E. Schmid, and K.-L. Kompa, J. Phys. Chem. **102**, 9334 (1998).
[27] N. A. Anderson, S. H. Pullen, L. A. Walker II, J. J. Shiang, and R. J. Sension, J. Phys. Chem. A **102**, 10588 (1998).
[28] https://slacportal.slac.stanford.edu/sites/lcls_public/instruments/amo/Documents/AMOtechspecs.pdf.
[29] See Supplemental Material at http://link.aps.org/supplemental/10.1103/PhysRevLett.108.253006 for more experimental and computational details.
[30] A. Eppink and D. Parker, Rev. Sci. Instrum. **68**, 3477 (1997).
[31] G. M. Roberts, J. L. Nixon, J. Lecointre, E. Wrede, and J. R. R. Verlet, Rev. Sci. Instrum. **80**, 053104 (2009).
[32] J. White *et al.* (to be published).
[33] C. Y. Ruan, V. A. Lobastov, R. Srinivasan, B. M. Goodson, H. Ihee, and A. H. Zewail, Proc. Natl. Acad. Sci. U.S.A. **98**, 7117 (2001).
[34] W. Fuss, W. Schmid, and S. Trushin, J. Chem. Phys. **112**, 8347 (2000).
[35] F. Tarantelli, A. Sgamellotti, L. S. Cederbaum, and J. Schirmer, J. Chem. Phys. **86**, 2201 (1987).
[36] S. Miyabe, C. W. McCurdy, A. E. Orel, and T. N. Rescigno, Phys. Rev. A **79**, 053401 (2009).
[37] A. Schlachter *et al.*, J. Phys. B **37**, L103 (2004).
[38] T. S. Zyubina, A. M. Mebel, M. Hayashi, and S. H. Lin, Phys. Chem. Chem. Phys. **10**, 2321 (2008).